Science Futures
2026, Vol. 2, No. 1, pp. 17–32
https://doi.org/10.11648/j.scif.20260201.12

Research Article

Projection of Climate Attributes Using CanESM2 RCM for the Lemo District of Central Ethiopia of Region

Alemgena Reta Nigussie[1, *], Dagnachew Daniel[1], Nebiyat Yilma[2]

[1]Weather/Climate Forecasting and Early Warning Department, Ethiopian Meteorology Institute, Hawassa, Ethiopia
[2]Meteorology and Hydrology Faculty, Water Technology Institute, Arba Minch, Ethiopia

Abstracts

This article assessed the historical climate attributes and the future projections for the Lemo district of south central Ethiopia based on the observed and the projected climate variables of the Meher season. An observation of rainfall, temperature, and down welling short wave radiation for the period 1991–2020 and climate projection data from the CanESM2 RCM for the period of 2021–2100 under the RCP4.5 and RCP8.5 were used. Model Bias Correction Method of capturing historical rainfall and temperature data for that specific area of study then correcting the bias found between the RCM data and observed station data. In our case, we have applied a scientific software called CMhyd (Climate Model data for hydrologic modeling) to extract the net CDF (Network Common Data Form) model data obtained from RCMs. Statistical tests and variability measuring indexes applied for analysis. Results showed insignificantly increasing trends of rainfall and temperature over the Lemo district during 1990 to 2020. And also the projections by 2021 to 2050 (near term), 2050 to 2080 (mid-term) as well as 2081 to 2100(end-term) indicate an increase in temperature compared to the 1991-2005 of baseline periods. Whereas high variability of rainfall amount, onset and cessation changes are expected to be happened in the future. This finding shows increasing trend of variability in rainfall and temperature indicating the risks of climate change impact. Therefore identifying relevant agricultural, environmental and social adaptation strategies are desirable.

Keywords

Climate Projection, Climate Change, Rain-fed Agriculture, RCM, Lemo District

1. Background

The Ethiopian cropping system mainly holds rain-fed, one-sided, and single cropping [1] has been vulnerable to the variability of seasonal onset and cessation of rainfall. Since cropping systems are not resistant to the changing climate, increasing food production sustainability has been in a longstanding challenge for smallholder farmers. Henceforth, as articulated by [2] agro ecological measures like diversification of cropping stems and integrated crop-livestock production systems applied as a good approach to strengthen climate change resilience.

The local temperature of the southern central Ethiopia categorized as tropical cold, hot, and temperate which is more controlled by elevation. Regardless of its climate characteristics, the region is vulnerable to risks of climate variability and change. Then, what makes it risky as considered by [3] farmland holding takes 0.1ha to 0.5ha for

*Corresponding author: nalemgena@gmail.com (Alemgena Reta Nigusse)

Received: 19 June 2025; **Accepted:** 3 November 2025; **Published:** 24 December 2025

46.5% of the farmers of the region followed by 25.4% of the total holders having 0.51 to 1 ha of land.

The increase in temperature trend caused by climate change encourages a favorable environment for weed and pest growth. In this region climatological onset of the rainy season starts at the end of February and early Jun. The earliest onset appears in the southwest and south-central parts and propagates to later dates in areas southern extreme. A revision report by [4] says the onset of the short rain season Belg (End-February, March, April, May) starts on March 1st dekade, and the cessation of summer rain (Jun, July, August, and September) just begin to uphold itself to October first dekade. The influence of rainfall, temperature, down welling short wave radiation, sowing date, and LRS is highest for the cropping system as [5] reported. Therefore, testified that the onset dates determines the sowing date, and the variability of minimum temperature is affected by down-welling short wave radiation. Such relations between cropping system and climate variables have paved the way for the application of climate projection data.

Most of the climate characterization research used a different to measure a change and Variability of climate analysis. However, this research attempts to detect climate variability and changes for the Lemo district using standard deviation, coefficient of variation, normalized anomaly regional index (RI) under the RCP4.5, and RCP8.5 scenarios of climate change.

2. Study Area and Methodology

Lemo district is 30 km to Hosanna town of Hadiya zone and 230km from Adis Ababa, which is located at 7o 64 ′N latitude and 37 ′89 ′E longitude with the area coverage of 354,368.77 Km-2 (Figure 1).

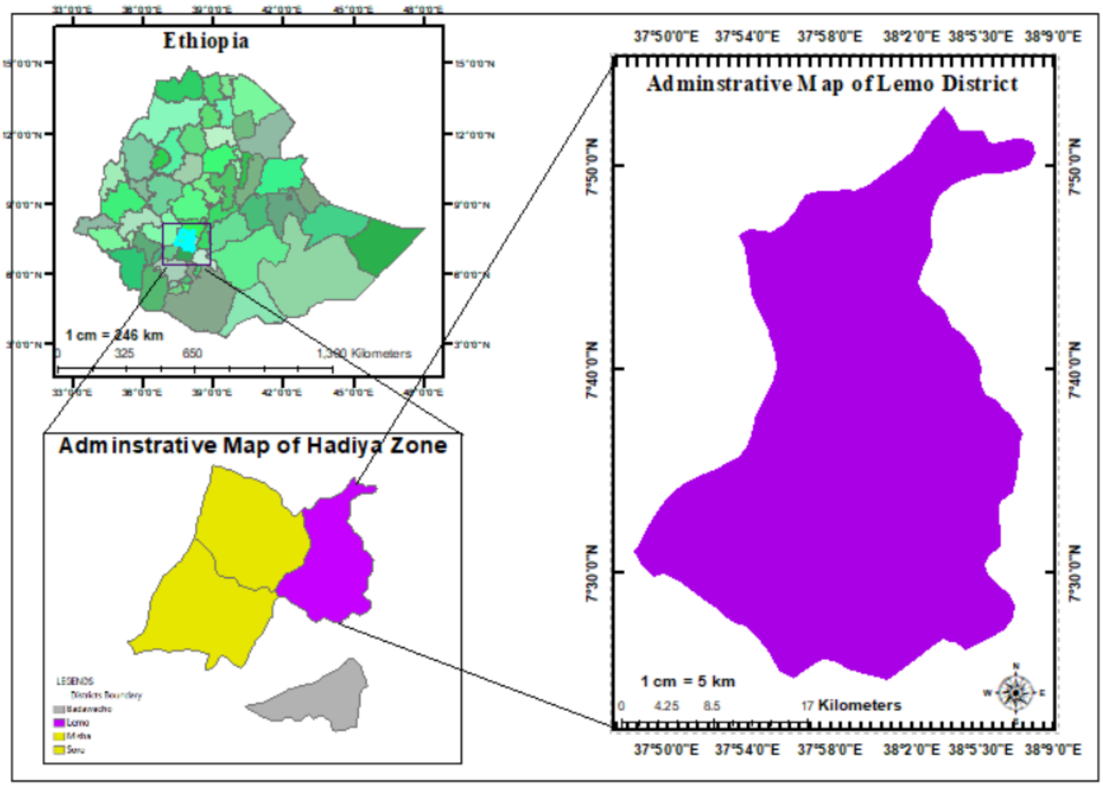

Figure 1. *location Map of the Lemo District.*

2.1. Method to Determine Trends by Modified Mann-Kendall Test

Modified Mann-Kendall test and Sen's slope estimator–trend detection, non-parametric Mann-Kendall test is widely used in detecting trends of variables in meteorology and hydrology fields Statistic S can be obtained by: -

$$S = \sum_{K=1}^{n-1} \sum_{j=k+1}^{n} sgn(Xj - Xk)$$

$$\mathrm{sgn}(\mathrm{Xj} - \mathrm{Xk}) = \begin{cases} +\ \mathrm{if}(\mathrm{Xj} - \mathrm{Xk}) > 0 \\ 0\ \mathrm{if}(\mathrm{Xj} - \mathrm{Xk}) = 0 \\ -1\ \mathrm{if}(\mathrm{Xj} - \mathrm{Xk}) < 0 \end{cases}$$

Where n is length of sample, Xk and Xj are from K = 1, 2…… n-1, j = K+ 1……n if n > 8 Statistics S approximates to normal distribution, the mean of S is 0 and the variance of S is given as follows: Var(S) = $\frac{n(n-1)(2n+5)}{18}$

Then the test statistics Z denoted by: -

$$Z = \begin{cases} \frac{S-1}{\sqrt{var(S)}}, \text{if } (S) > 0 \\ \text{if } (S) = 0 \\ \frac{S+1}{\sqrt{var(S)}}, \text{if } (S) < 0 \end{cases}$$

If Z > 0 it is Increasing Trend
If Z < 0 it is Decreasing Trend and
If Z = 0 it is Indifference [6]

2.2. Methods to Measure a Change and Variability

Through composing the raw data of rainfall, temperature and evaporation in a tabular way, we have arranged and organized in suitable form for analysis by extracting the monthly total rainfall, total annual rainfall as well monthly mean temperature. Here, we analyze the impact of intra-seasonal and inter-seasonal climatic variability on crop yields. Thus, apart from measuring the strength of climate variability this study tries to capture the direct and indirect effects of temperature, rainfall and evaporation to wheat and maize yield. It has measured by the seasonal coefficient of variation (CV) calculated as the ratio of the standard deviation to the mean of each climate variables. Seasonal and annual variability of these variables in both districts has analyzed using standard deviation in equation (1) coefficient of variation in equation (2) and normalized anomaly in equation (3) for instance applied by [7]. The formula for the Standard deviation is:-

$$SD(S) = \sqrt{\frac{\Sigma(Xi-\overline{X})}{(n-1)}} \quad (1)$$

Where: - SD is Standard Deviation
-Xi is monthly total rainfall or monthly Mean Temperature
-X Is Mean Annual Rainfall or Annual Mean Temperature
-N is total Amount of Annual Rainfall or Temperature the formula for Coefficient of variation is:

$$CV = \frac{SD}{\overline{X}} \text{ x } 100 \quad (2)$$

Finally, the predictable dispersion or standard deviation (SD or S) can be calculated as: - When the CV values < 20% indicates less variable, when 20% < CV < 30% indicates moderately variable while CV > 30% is highly variable [8].

Normalized Anomaly or Regional Index (RI) of variability [9]

$$RI = \frac{Xi-\overline{X}}{S} \quad (3)$$

$$\text{Percent of Change} = \left(\frac{\text{Observed}}{\text{Projected}} - 1\right) * 100$$

2.3. Method to Estimate Evapotranspiration

Hargreaves-Samani Method: -developed an expression to estimate ETo as a function of the solar radiation that reaches the ground level and the mean temperature of the air which is defined as: -

$$PET = 0.000938Ra\ (Tmean + 17.8)\sqrt{(TMX - TMN)}$$

Where: - Ra is the net radiation received at the highest level over the study area in Kj/m2day-1,

- T mean is the mean daily temperature in ℃ in the study area.

2.4. Methods of RCM Performance Evaluation

R-Squared: This is probably the most commonly used statistics and allows us to understand the percentage of variance in the target variable explained by the model. It has computed as a ratio of the regression sum of squares and the total sum of squares.

$$\mathcal{R}^2 = \frac{\sum_{i=1}^{n}(Oi-Om)(Si-Sm)^2}{\sum_{i=1}^{n}(Oi-Om)^2 * \sum_{i==1}^{n}(Si-Sm)^2}$$

$$MBE = \sum_{i=1}^{n}\frac{(Si-Oi)}{n}$$

RMSE: A metric that tells us how far apart the predicted values are from the observed values in a dataset, on average. The lower the RMSE, the better a model fits a dataset.

$$RMSE = \sqrt{\left(\frac{(Si-Sm)^2}{n}\right)}$$

Where: - n is the number of observations, Si is simulated, oi is the observed, Om is the observed mean, and Sm is the simulated mean grain yields.

2.5. Method of RCM Bias Correction

The representativeness of RCM for a single specific location in a globe by the system called Model Bias Correction Method of capturing historical rainfall and temperature data for that specific area of study then correcting the bias found between the RCM data and observed station data. In our case, we have applied a scientific software called CMhyd (Climate Model data for hydrologic modeling) to extract the net CDF (Network Common Data Form) model data and bias-correct the data obtained from RCMs. The historical observed data from 1990-2020 for the typical stations Butajira of Mesqan district and Hossana of Lemo district and historical RCM from 1991-2005 has used for comparison that will be discretely corrected by statistical approaches established in CMhyd tool.

Table 1. *Types and sources of enrolled RCM Models.*

No.	Types of RCMs	Institute (Center of Models)	Driving GCMs	References
1	Can ESM2-AFR22	Cape Town-South Africa	CORDEX-AFRICA	Alexandro Dosio, 2011, Jury M. W, 2021
2	CGM3-MPI	Max-Plank Institute of Meteorology, Germany	MPI-M-MPI-ESM-LR	Dibaba et al., 2019 and Endris et al., 2013
3	REMO-MPI	Max-Plank Institute of Meteorology, Germany	MPI-M-MPI-ESM-LR	Assamnew and Tsidu, 2020

2.6. Processing of Bias Correction

CMhyd designed to provide simulated climate data that considered representative for the location of the gauges used in a watershed model setup. Therefore, climate model data has extracted and bias-corrected for each and specific gauge locations i.e. 080 07' 21.4" N latitude and 0380 22' 33.4" E longitude for station Butajira and 070 34' 41" N latitude and 0370 51' 22.1" E longitude for station Hosanna of their specific district.

Linear Scaling Additive and Multiplicative Bias Correction Method

There are several bias correction methods, which has developed to downscale climate variables from the RCMs, ranging from the simple scaling approach to sophisticated distribution mapping [10]. Evaluating and finding the appropriate bias correction method is necessary to assess climate change signals reflected to crop production. So, the approaches of linear scaling - additive and multiplicative bias correction methods for temperature and for precipitation respectively used in this process. Because (1) the method uses a constant correction factor estimated by the difference between RCM simulation data and observed station data for each calendar day. (2) It needs a data on a daily-observed station and historical RCM data.

The future time series projection of climate is downscaled using the correction factors called overlap period (the years found between 1991-2005 historical RCM and 1990-2020 observed station data) and base line period (1991-2005 historical RCM).

3. Rainfall Variability and Trend of Lemo District

Lemo district has two meteorological stations called Hossana and Fonko characterized by the combined length of *belg* (March-May) and *kiremt* (Jun-September) known as "MEHER".

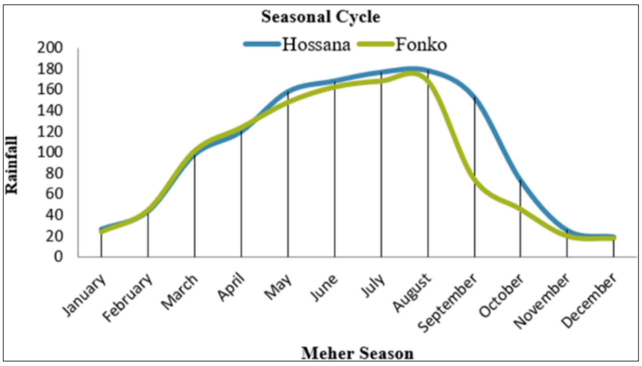

Figure 2. *Seasonal Cycle of the Lemo district.*

The main peak rainfall recorded in July and August for both stations but the lowest is in March. Consequently, the rainy season is arranged from March to October at that point crop calendar for Meher wheat production has been reserved from it. This is straight with the Ethiopian crop calendar of main crops, developed by [11].

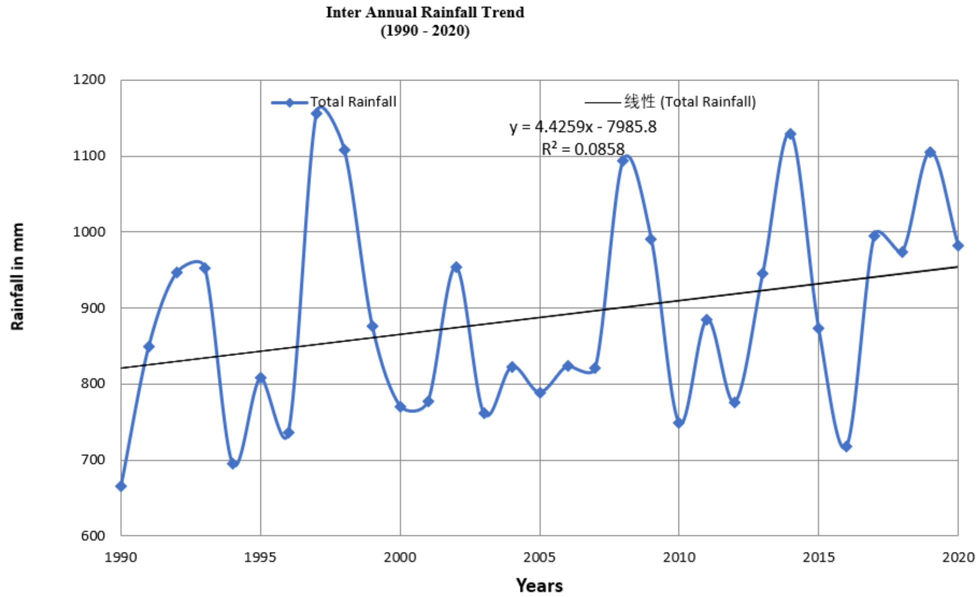

Figure 3. Annuall Rainfall trend of the Lemo district.

Table 2. Monthly Rainfall trends and variations.

No.	Crop Calendar	Monthly Mean RF	SD	(CV in %)	MK	SS	Trend Level
1	March	103.4	7.3	43.2%	0.12	0.10	↑
2	April	144.2	66.0	44.3%	0.13	0.11	↑
3	May	161.8mm	68.5	43.8%	0.11	0.94	↑
4	Jun	109.3mm	66.8	27.4%	0.13	0.77	↑
5	July	158.1mm	65.0	42.5%	0.07	0.55	↑
6	August	185.9mm	63.9	27.2%	0.14	0.79	↑
7	September	76.5mm	59.8	33.2%	0.21	1.14	↑
8	October	32.6mm	58.8	44.7%	0.06	0.73	↑

SD-standard deviation, CV-coefficient of variation, MK is Mann–Kendall trend test, SS (Sen's slope) is the change in (mm)/annual; **: α = 0.01; *: α = 0.05; †: α = 0.1 level of significance.

The Mann-Kendall test emphasizes that the monthly rainfall in Hosana station has an increasing trend during 1990-2020. According to [12] the variability shows CV > 30% highly variable pattern of rainfall across the months except Jun and August (Table 2).

The annual, monthly, and daily temperature data for the climate period of 1990 - 2020 were undertaken to detect the temperature trend and variability in the Lemo district.

Table 3. Monthly Temperature trends and variations.

No.	Crop Calendar	Mean Minimum Temperature	MK	SS	Trend Level	Mean Maximum Temp.	MK	SS	Trend Level
1	March	11.3 ℃	0.35	0.03	↑	23.1 ℃	0.33	0.03	↑
2	April	11.5 ℃	0.35	0.03	↑	21.5 ℃	0.27	0.04	↑

No.	Crop Calendar	Mean Minimum Temperature	MK	SS	Trend Level	Mean Maximum Temp.	MK	SS	Trend Level
3	May	11.3 ℃	0.42	0.03	↑	20.2 ℃	0.32	0.05	↑
4	Jun	11.5 ℃	0.40	0.03	↑	20.3 ℃	0.24	0.04	↑
5	July	11.0 ℃	0.45	0.04	↑	21.4 ℃	0.12	0.01	↑
6	August	10.9 ℃	0.21	0.03	↑	22.7 ℃	0.57	0.05	↑
7	September	10.4 ℃	0.28	0.04	↑	23.4 ℃	0.35	0.05	↑
8	October	9.8 ℃	0.11	0.04	↑	23.5 ℃	0.30	0.02	↑

SD-standard deviation, CV-coefficient of variation, MK is Mann–Kendall trend test, SS is Slope (Sen's slope) is the change in (mm)/annual; **: α = 0.01; *: α = 0.05; †: α = 0.1 (Level of Trend).

The trend test of mean temperatures has been significantly increasing over time. The monthly minimum temperature is increasing by 0.01 ℃ – 0.05 ℃ for maximum temperature ranges from 0.03 ℃ – 0.04 ℃ with its monthly mean of increase by the slop of 0.03 to 0.12. The monthly minimum temperature trend shows a different outcome than the maximum one.

The seasonal onset, cessation, and LGP characters for the Hosanna station found in the Lemo district are characterized by the earliest onset dates of March 7 and late-onset on April 26.

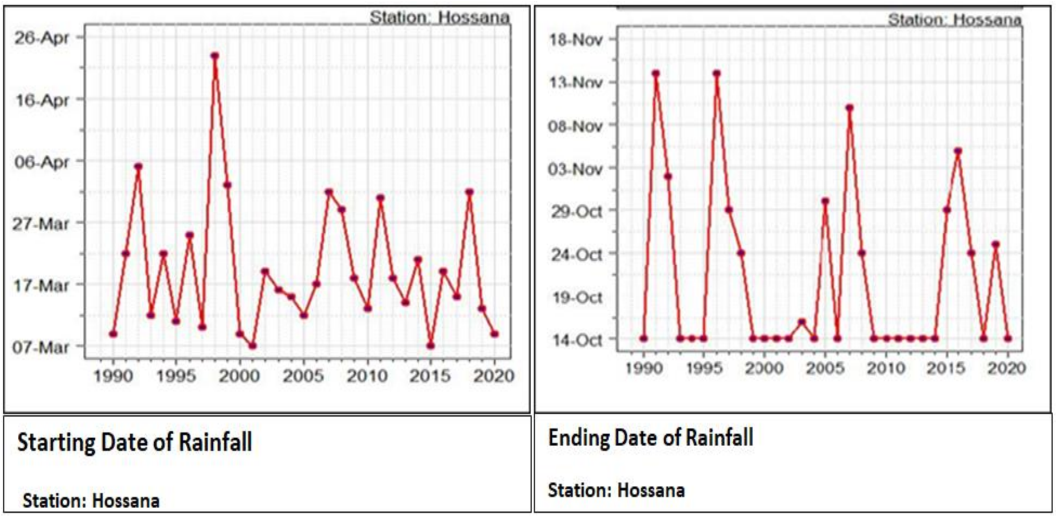

Figure 4*. Rainfall Onsets and Cessation date of the Lemo district.*

Besides the bimodal type-II pattern of rainfall, the cessation date is established on October 14 with its much later up to November 13. The length of the growing period with shorter growing period observed in 1998 about 180 days. The longest growing period in the district was observed in 2016 which is about 249 days. So Lemo districts have a productive LGP in a range of 180 days to 249 days with a 17% variation from the mean.

4. Discussion

4.1. Projection of Climate Attributes from 2021-2100 on RCP4.5 and RCP8.5

To provide sound meteorological input for climate impact studies it is important to address the uncertainty induced by climate simulation models. Here we tried to present the result of statistically evaluated RCMs such as CanESM2, CGCM3-MPI, and REMO-MPI for rainfall.

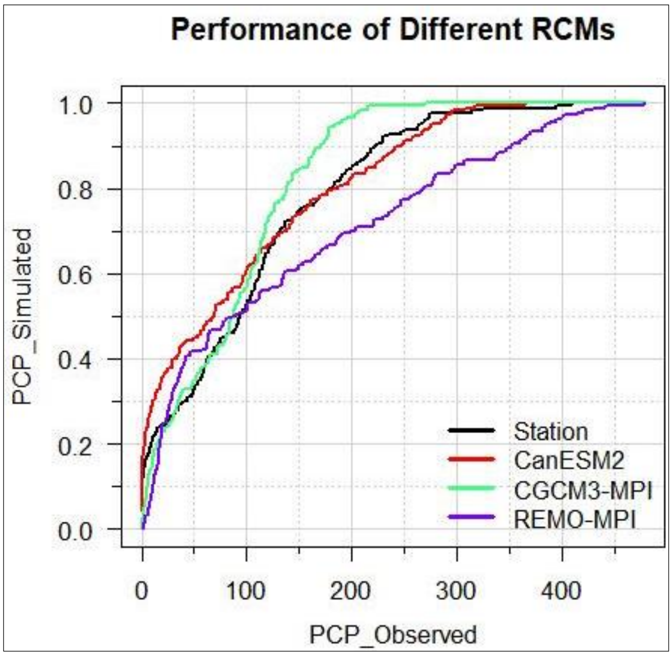

Figure 5. Validation Performance of Different RCMs.

The presented result shows lower clear projection for both REMO-MPI and CGCM3-MPI, whereas coherent projection has been seen in an RCM CanESM2 with the observed station data.

Table 4. Correlation Performance of Enrolled RCMS.

	CanESM2	CGCM3-MPI	REMO-MPI
CORR	0.633	0.597	0.582
BIAS	0.915	0.842	1.344
PBIAS	8.485	-16.793	34.361
ME	8.616	-17.052	34.892
RMSE	97.285	72.492	112.179

Historical RCM rainfall data from different sources of institutions for the data sets of 1991-2005 were collected and evaluated against the observed ground-based rainfall stations for the period 1990 to 2020 of our case. The statistical depths of fitness show that the two models CGCM3-MPI and REMO-MPI did not achieve to generate a better-performed outcrop sufficiently. The correlation coefficient realized by the CGCM3-MPI and REMO-MPI is 0.597 and 0.582 respectively, but the CanESM2 model gets up to 0.633-correlation by the rainfall data

4.2. Projected Annual Rainfall Change on RCP4.5 Scenario

The projection of rainfall for station Hossana manifests a systematic increase of rainfall for the coming 80-year period on RCP 4.5. It will show an increasing trend starting up to the end term of 2100 then it will intensify from 2050-2080 up slop of ascend (Figure 6). Such a parallel trend of two terms implies the fact that rainfall probability and frequency over the station shifted temporally following the changing climate on RCP 4.5.

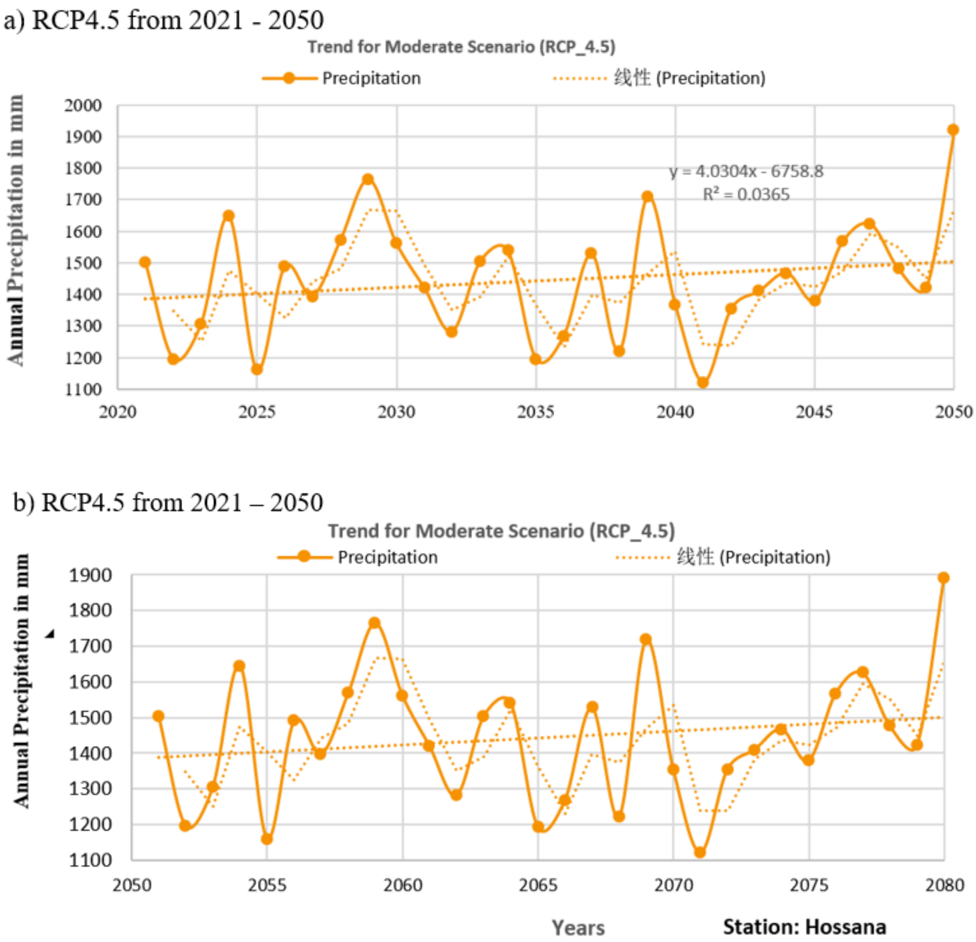

Figure 6. a) and b) Future Annual Rainfall trend on RCP4.5.

4.3. Projected Annual Rainfall Change on RCP8.5 Scenario

The rainfall trend test has performed a decreasing pattern for the coming two terms of climate periods and starts to increase beginning from the midterm period under RCP8.5. Moreover, a considerable decreasing trend of rain for the near term (2021-2050) vanishes from 2030 to 2050. It will take the sinusoidal pattern of increasing from 2055 up to the end of 2080 (Figure 7). This will be a change in the intensification of the two-weather extremes drought and flooding respectively in the near-term to mid-term period of the RCP8.5 emission scenario.

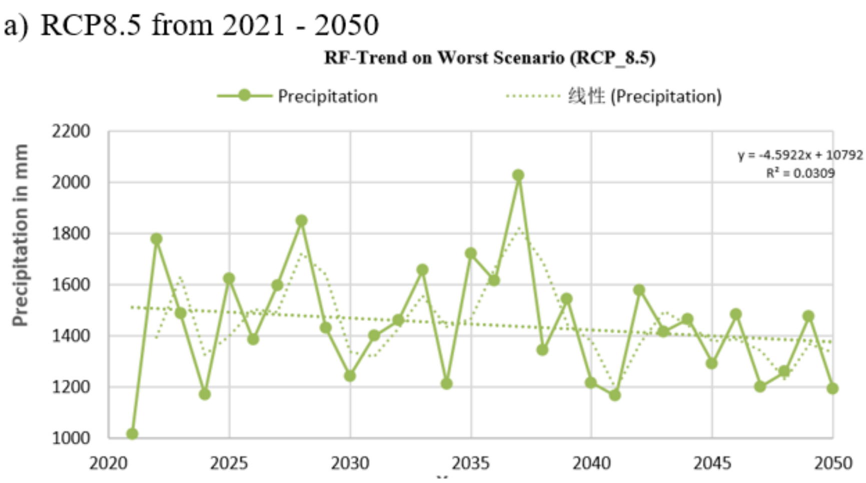

b) RCP8.5 from 2051 - 2080

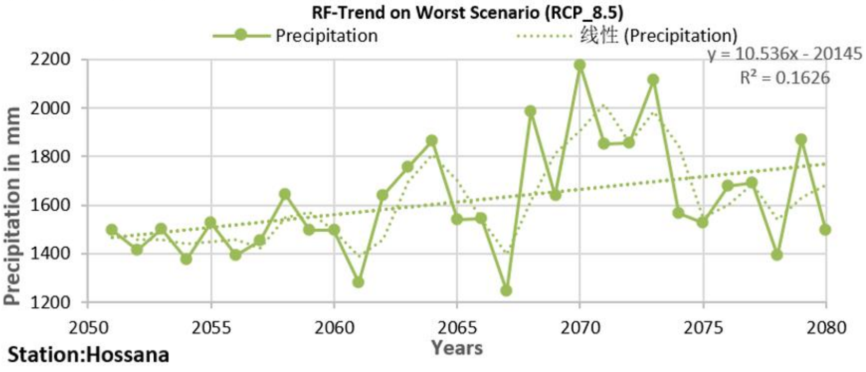

Figure 7. *a) and b) Future Annual Rainfall trend on RCP8.5.*

4.4. Projected Annual Temperature Trend on RCP4.5 and RCP 8.5 Scenario

The long-term differences in mean annual temperature will show an inter-annual trend up to the end of 2080. The minimum temperature will show an increasing slope of 0.080C per annum starting from the near-term to mid-term period, which implies the presence of a global warming trend.

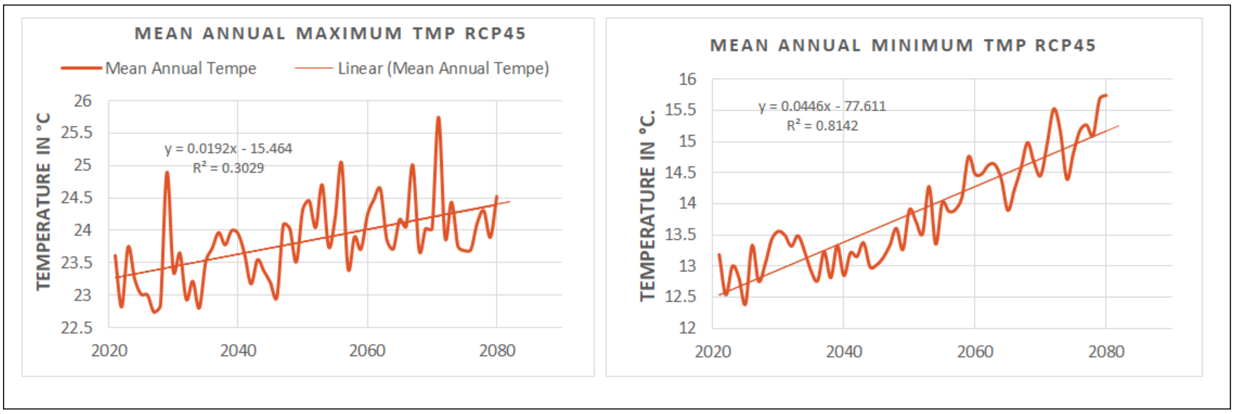

Figure 8. *Future Annual Maximum and Minimum temperature trend on RCP4.5.*

The overall annual temperature trend significantly attributed to the minimum temperature increase. The rate of change in minimum temperature measured by 0.07 ℃ to 0.045 ℃ per decade during on RCP4.5 and RCP 8.5.

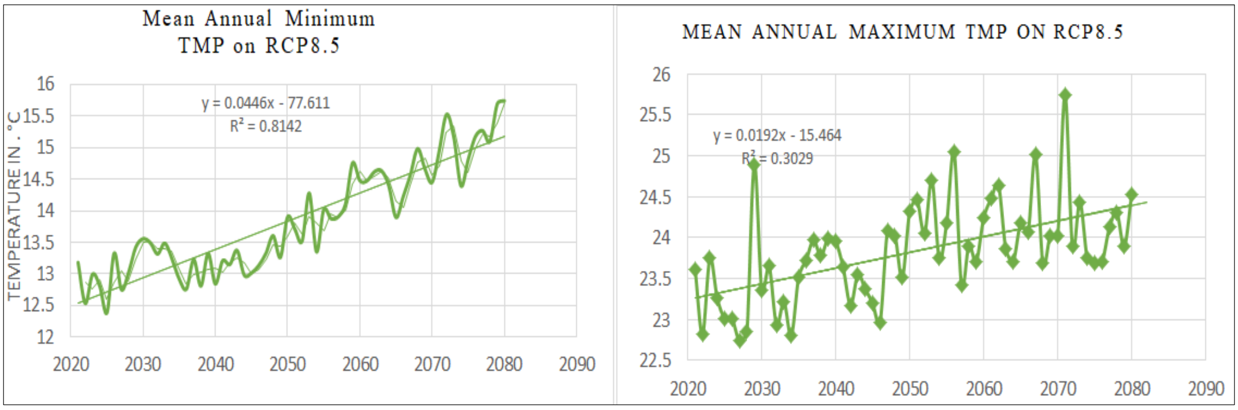

Figure 9. *Future Annual Maximum and Minimum temperature trend on RCP8.5.*

The result of the projection for temperature trend reveals a significant change in both scenarios over Hossana station. (Figure 9) shows, the acquired temperature trend in an increasing manner in the range of 0.021° to 0.045℃ every decade of 2050s and 2080s on RCP 4.5 scenario. The trend for maximum temperature indicates a moderate increasing.

4.5. Projected Annual Rainfall and Temperature Change for the Period of (2081-202100)

The rainfall and temperature trend has ended in an increasing and decreasing pattern for the single terms of climate period from 2081-2100. This will start to increase in rainfall for both scenarios of RCP4.5 and RCP8.5. Whereas the minimum temperature under RCP4.5 indicates a decreasing pattern different from RCP8.5.

Table 5. *Future Rainfall and Temperature trends (2081 - 2021).*

RCPs	End Term	Variable	Corrected Z-(MK)	P-value	Variance (V)	Sen's slope (SS)	Level of Trend
RCP 4.5	2081-2100	Rainfall	0.081	0.93	8.09	0	↑
RCP 8.5	2081-2100	Rainfall	1.02	0.30	9.29	8.49	↑
RCP 4.5	2081-2100	TMN	-1.03	0.30	3.13	-2.35	↓
RCP 8.5	2081-2100	TMN	5.44	5.17	2.39	0.00	↑
RCP 4.5	2081-2100	TMX	-0.36	0.71	1.24	-8.87	↓
RCP 8.5	2081-2100	TMX	1.34	0.33	-6.38	0.00	↑

V-coefficient of variation, MK is Mann–Kendall trend test, SS is Slope (Sen's slope) is the change in (mm)/annual; **: α = 0.01; *: α = 0.05; †: α = 0.1 level of significance (Level of Trend).

The rainfall and temperature trend test has ended in an increasing and decreasing pattern for the single terms of climate period from 2081-202. This will start to increase in rainfall for both scenarios of RCP4.5 and RCP8.5. Whereas the minimum temperature under RCP4.5 indicates a decreasing pattern that is different from RCP8.5. Moreover, a significant decreasing trend of maximum temperature was observed on RCP4.5 and increasing on RCP8.5 Table 4.10. The level of trend for the Lomo district will reveal an increasing step of downwelling short wave radiation on both RCP4.5 and RCP8.5 during the end-term scenario. The remaining two terms of the climate change scenario will take the decreasing level of trend (Table 5).

Table 6. *Future Down welling Shortwave Radiation trends (2081 - 2021).*

Trends in a Down welling short wave Radiation					
Terms of Scenario	**MK-Value (Zc)**	**P-value**	**Sen's slope**	**Level of Trend**	**Amount (Qs) in KJ/M2**
RCP4.5_NT	-2.70	0.01	0.00	↓	37.13
RCP8.5_NT	-0.32	0.75	0.00	↓	33.17
RCP4.5_MT	-0.78	0.43	0	↓	19.55
RCP8.5_MT	-2.03	0.04	0	↓	19.29
RCP4.5_ET	1.81	0.07	0.00	↑	54.39
RCP8.5_ET	0.67	0.50	0.00	↑	64.11

The amount and trends of DWSWR (Downwelling short wave Radiation) (Qs) might be the image for the earthly position of the district found. This implies that the tropical Africa area will obtain an energy surplus which will in turn release higher water vapor of atmospheric greenhouse gas reducing the future DWSWR received by the crop land. In the case of wheat crops, the projected DWSWR amount characterizes a sinusoidal way of increment throughout the entire period from near-term to end-term. The largest amount of DWSWR during the near-term starts to decrease from 37.13 KJ/M2 to 19.55 KJ/M2 it will begin its increment up to 64.11 KJ/M2 during the end-term period.

4.6. Projected Onset Date and Cessation Dates on RCP 4.5 Scenario (2021-2100)

Prediction of onset and cessation dates as [13] (Nicholson, S. E. (2017). Climate and climatic variability of rainfall over eastern Africa. Reviews of Geophysics, 55(3), 590-635).

Says, have usually assumed less emphasis than the seasonal forecast of climate, especially in the East African scientific community. Because of that, the grassroots climate service has been forced to expect abnormal determination of onset and cessation date from the operational ECMWF (European Centre for Medium-Range Weather Forecasts) seasonal forecast model. The exact timing of LRS for the on both RCPs will show a deviation from its baseline period.

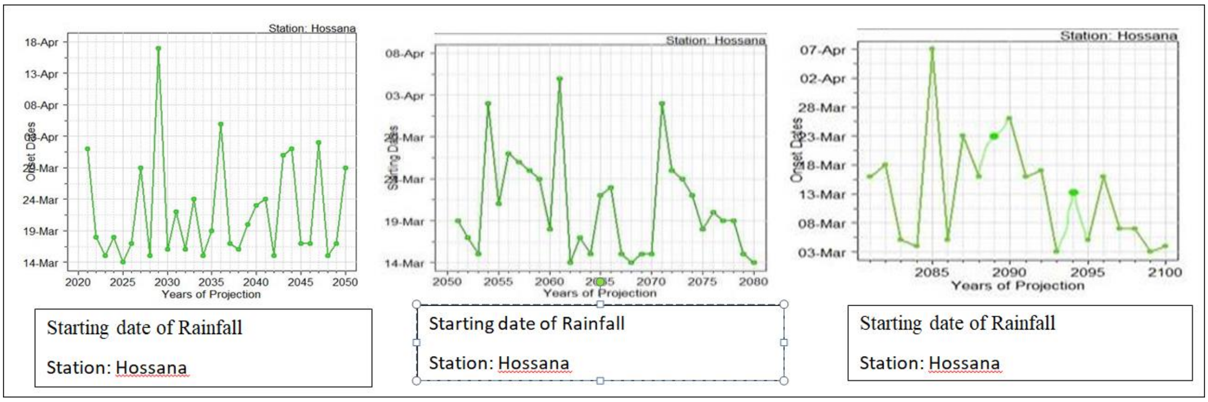

Figure 10. *Future Onset date on RCP 4.5.*

Henceforth, the projection of onset dates will be by a late start of rainfall as compared to the base period on both RCP 4.5 and RCP 8.5. The projection on RCP 4.5 for the near-term period, the rainfall starts in 2nd decade of April. For the next two climate periods, the earliest starting date will be from March 17 and the latest possible starting date will be 16 April 2029 (Figure 10).

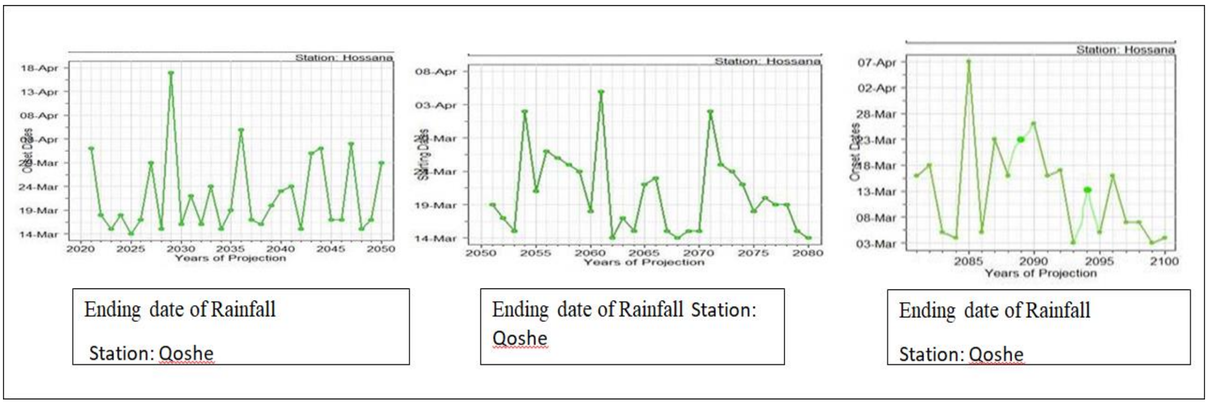

Figure 11. *Future Cessation date on RCP 4.5.*

4.7. Onset Date and Cessation Date of Rainy Season on RCP 4.5 Scenarios (2021-2100)

The mean starting date will have a smaller deviation (SD) of 7 days, from the mean starting date of 22 March. It suggests that there will be a more constant pattern with a lower risk of overtaking agricultural activities.

Table 7. *Analysis of Onset date variation from the baseline (2021 - 2021).*

	Hossana on RCP 4.5			
Analysis	**Onset Date Baseline**	**Near-Term**	**Mid-Term**	**End-Term**
MEDIAN	March 17	April 15	March 17	16 April
SD	7-days	5	7	7
CV (%)	35	31	37	63

The earliest end date for a near-term period on RCP 4.5 will be expected on October 7 in most years. The end date for the mid-term period (2050-2080) will be extended to the end of 10th November. During the end-term (2081-2021), most of the cessation dates will stay from October 16 to November 15. The deviation will be 7 days later and forth with a 29% variation by a lower variability and risks of cropping.

Table 8. *Analysis of Cessation date variation from the baseline on RCP4.5.*

	Hossana on RCP 4.5			
Analysis	**Cessation Date Baseline**	**Near-Term**	**Mid-T erm**	**End-Term**
AVG	19	10	10	16
MEDIAN	19	7	7	16
SD	8	7	9	7
CV	44	29	65	42

4.8. Projected Onset date, Cessation date, and LRS on RCP8.5 Scenario

The starting date of the Meher season on RCP 8.5 (2050-2080), drops on 11th March with a variation of 17 days later and forth from the mean date (Figure 12).

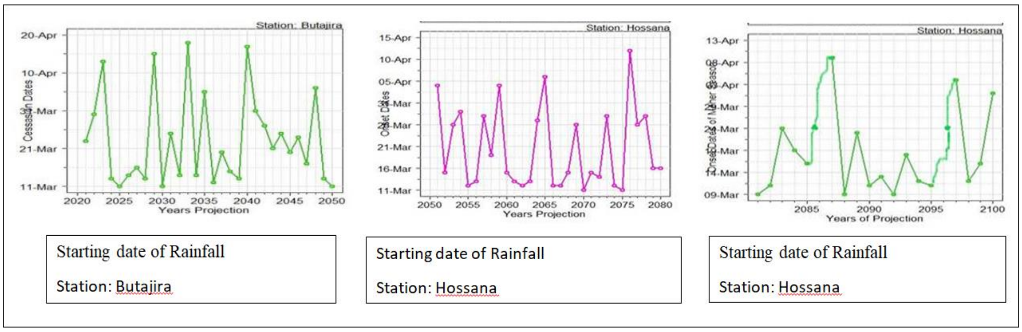

Figure 12. *Future Onset date on RCP 8.5.*

There will a higher standard deviation of SD =11 in the projection of near-term and mid-term periods with a variation of 57% and 64% respectively from the baseline. Likely climatic conditions could not be controlled and agricultural activities will be at a higher risk (Table 9).

Table 9. *Analysis of Onset date variation from the baseline on RCP8.5.*

		Hossana on RCP 8.5		
Analysis	**Onset Date Baseline**	**Near-Term**	**Mid-T erm**	**End-Term**
AVG	21	March 19	March 17	March 14
MEDIAN	17	20	16	13
SD	7	11	19	17
CV	35	57	64	51

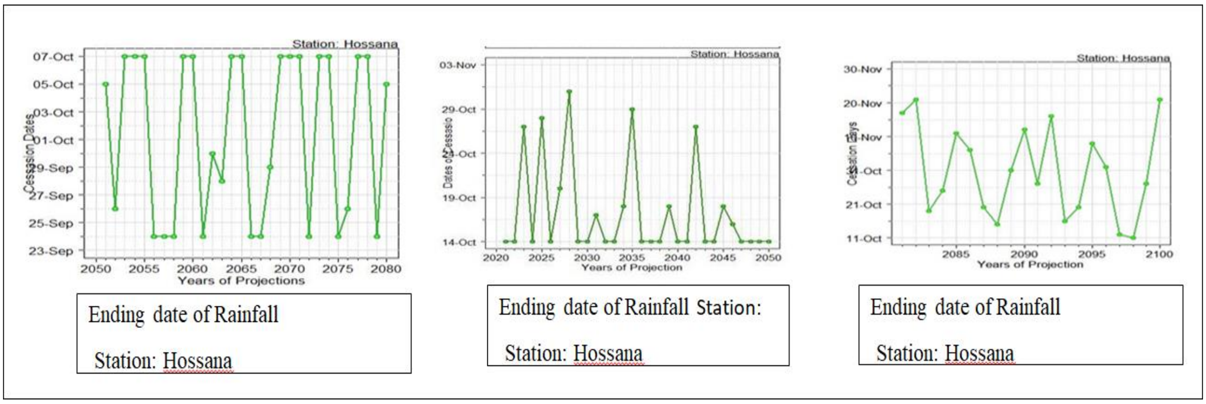

Figure 13. *Future Cessation date on RCP 8.5.*

The latest end date of the season as it pertains in (Figure 13) will drop on 7th October for the climate period of 2050-2080 on RCP 8.5 scenario. Whereas 23rd September will be the earliest end date of the season with a variation of 61% from the mean with a higher seasonal and risk.

Table 10. *Analysis of Cessation date variation from the baseline on RCP8.5.*

		Hosanna on RCP 8.5		
Analysis	**Cessation Date Baseline**	**Near-Term**	**Mid-T erm**	**End-Term**
AVG	19	October 15	September 26	October 18
MEDIAN	19	14	14	19
SD	8	9	11	8
CV	44	60	71	45

The standard deviation in the mid-term period of projection is SD = 11 characterized by a 71% variation of cessation date from the baseline. October 14th to November 3rd will be the earliest and latest ending dates of the rainy season respectively for the near-term climate period.

4.9. Projected Length of Rain Season (LRS) for the Lemo on RCP 4.5 and RCP 8.5 Scenario

The shortest growing period on RCP 4.5 takes an average of 197 days in the end-term period and the longest LRS 242 days in the mid-term with a minimum of 18% variation from the average baseline LRS.

Table 11. *Analysis of LRS variation from the baseline on RCP4.5.*

	LRS for the Hossana Station on RCP 4.5			
Analysis	**LRS_Baseline**	**LRS_Near-Term**	**LRS_Mid-Term**	**LRS_End-Term**
AVG	200	204	231	197
MEDIAN	208	205	242	212
SD	55	49	41	47
CV	28	23	18	21

Depending on the genotype of leaf appearance and floral differentiation for the different crops, induced by photoperiod determine the number of days from emergence to physiological maturity in the field.

Table 12. *Analysis of LRS variation from the baseline on RCP8.5.*

	LRS for Hossana Station on RCP 8.5			
Analysis	**LRS_Baseline**	**LRS_Near-Term**	**LRS_Mid-T erm**	**LRS_End-Term**
AVG	200	214	241	187
MEDIAN	208	215	252	202
SD	55	59	43	47
CV	28	28	18	25

The shortest length os rain season of 161 days and the longest through 253 days, from the average of 200 days on the RCP 8.5 scenario. In Lemo district land preparation takes place during the first 30 to 50 days before the main cropping season, the average LRS extends up to 207 days with a variation of 22% indicating substantial grain productivity in the area. In addition to that, for the coming 80 years the production of wheat cultivars the longest and shortest LGP spreads up to 265 in 2072 and 174 days in 2042 respectively.

5. Conclusion

A significant temporal variation in rainfall and temperature shows a changing trend during the climate periods of study 1990-2020 for the Lemo district. The spatial-temporal rainfall of double pick, which attains from March to May as a smaller and June to October as a higher and longer range has taken as a single cropping season by the agronomist's terminology called "MEHER". It can gain 770mm of seasonal rainfall which decreases by 23% and 21% in average per season. The average seasonal minimum temperature of 11℃ & maximum temperature of 22℃ is increasing by the rate of change near 0.058℃, 0.06℃, 0.087℃, 0.09℃, 0.17℃, 0.11℃, 0.12℃ and 0.029℃ per each month respectively during 1990–2020. The seasonal variability and change gets a likely 4 to 5-week fluctuation in its onset and 3 to 4 weeks' fluctuation in its cessation from the exact planting dates 21st April of Meher cropping season.

The projected changes in rainfall of the district as compared to baseline period reflect its own specific character in the two scenarios of RCP4.5 and RCP8.5. For instance, the future rainfall change of Lemo district for the coming 80-years will decrease by 27% to 33% on RCP4.5 scenarios but, a decline by 20% to 60% on RCP8.5 scenarios. The change in temperature compared to baseline period will share a common increasing movement by the rate of 0.30℃ to 0.81℃ increasing on both of RCP4.5 and RCP8.5 scenarios of climate change.

There will a deviation of 6-days to 13-sdays from the baseline onset date 19th April which will show a -14% to 42% for from the baseline. The cessation date will shows 7-day late from baseline date of cessation with a lower risk of cropping system. Whereas, on RCP8.5 scenario 11-days to 13-days variation of onset from baseline date 19th April for cropping will fall on a range a moderate risk of cropping activities.

6. Recommendation

1) From the analysis of inter-seasonal climate variability in Lemo district 5th April is the best time of cropping. During this period suitable weather condition is available with the 21st April to mid-May is the best period of cropping with the a suitable weather condition of TAV = 180C, Down welling short wave radiation (DWSWR↓) =23.4mJm-2 and RF = 3.7mm per day as we analyzed.
2) From the repeated output, since the last few years the rainfall starts late and ends early with a shortened LGP, this shows the need for adapting short growing crops in both districts.

Abbreviations

CanESM2	Second Generation Canadian Earth System Model
RCM	Regional Climate Model
RCP	Representative Concentration Pathway
RCP4.5	A medium-level Mitigation Emission Scenario
RCP8.5	A high-level, Business-as-usual Emission Scenario
CMhyd	Climate Model Data for Hydrologic Modeling
CDF	Network Common Data Form (Common Data Format)
CV	Coefficient of Variation
RI	Regional Index (Normalized Anomaly)
PET	Potential Evapotranspiration
ETo	Reference Evapotranspiration
MBE	Mean Bias Error
RMSE	Root Mean Square Error
GCM	Global Climate Model
CORDEX	Coordinated Regional Climate Downscaling Experiment
MPI	Max Planck Institute
CGCM3	Third Generation Coupled Global Climate Model
REMO	Regional Model
LR	Low Resolution
SD	Standard Deviation
MK	Mann-Kendall (trend test)
SS	Sen's Slope
LGP	Length of Growing Period
LRS	Length of Rainy Season
CORR	Correlation Coefficient
PBIAS	Percent Bias
ME	Mean Error
TMN	Minimum Temperature
TMX	Maximum Temperature
DWSWR	Downwelling Short Wave Radiation
Qs	(Symbol for DWSWR amount)
ECMWF	European Centre for Medium-Range Weather Forecasts
NT	Near-Term
MT	Mid-Term
ET	End-Term
AVG	Average
MEDIAN	Median
TAV	Average Temperature
RF	Rainfall
FAO	Food and Agriculture Organization of the United Nations

Authors Contributions

Alemgena Reta Nigusse: Conceptualization, Data curation, Methodology, Software, Writing–original draft, Investigation, Funding acquisition, Resources, Writing – review & editing

Dagnachew Daniel: Supervision, Project administration, Visualization, Validation, Writing – review & editing

Nebiyat Yilma: Data curation, Formal analysis, Writing – review & editing

Conflicts of Interest

The authors declare no conflicts of interest.

References

[1] Adenle, A. A., Ford, J. D., Morton, J., Twomlow, S., Alverson, K., Cattaneo, A, ... & Ebinger, J. O. (2017). Managing climate change risks in Africa-A global perspective. *Ecological Economics*, *141*, 190-201.

[2] Duru, M., Therond, O., Martin, G., Martin-Clouaire, R., Magne, M. A., Justes, E., ... & Sarthou, J. P. (2015). How to implement biodiversity-based agriculture to enhance ecosystem services: a review. *Agronomy for sustainable development*, *35*, 1259-1281.

[3] Workayehu, T. (2014). Legume-based cropping for sustainable production, economic benefit and reducing climate change impacts in southern Ethiopia. Journal of Agricultural and Crop Research, 2(1), 11-21.

[4] Wakjira, M. T., Peleg, N., Anghileri, D., Molnar, D., Alamirew, T., Six, J., & Molnar, P. (2021). Rainfall seasonality and timing: implications for cereal crop production in Ethiopia. Agricultural and Forest Meteorology, 310, 108633.

[5] Mateos, L., López-Cortijo, I., & Sagardoy, J. A. (2002). SIMIS: the FAO decision support system for irrigation scheme management. *Agricultural Water Management*, *56*(3), 193-206.

[6] Hamed, K. H., & Rao, A. R. (1998). A modified Mann-Kendall trend test for autocorrelated data. *Journal of hydrology*, *204*(1-4), 182-196.

[7] Zeleke, T., Giorgi, F., Mengistu Tsidu, G., & Diro, G. T. (2013). Spatial and temporal variability of summer rainfall over Ethiopia from observations and a regional climate model experiment. Theoretical and applied climatology, 111(3), 665-681.

[8] Yehualaw, E., Haile, T., Mickus, K., Beardsmore, G., & Nigusse, W. (2024). Electrical resistivity and magnetic methods in mapping groundwater on the western margin of the Central Main Ethiopian Rift-A case study in the Belesa area, eastern Lemmo Woreda, Ethiopia. Acta Geodaetica et Geophysica, 59(4), 441-461.

[9] Nouaceur, Z., Murarescu, O., & Muratoreanu, G. (2025). The Investigation of Trends and Wet and Dry Rainfall Cycles in North Africa (In Morocco, Algeria, and Tunisia)(1970–2023). Geosciences, 15(3), 80.

[10] Teutschbein, C., & Seibert, J. (2012). Bias correction of regional climate model simulations for hydrological climate-change impact studies: Review and evaluation of different methods. Journal of hydrology, 456, 12-29.

[11] Gebru, B., Kwena, K., Mworozi, E., & Sewankambo, N. (2023). Scaling-up pathways of last mile climate information services for community resilience in Uganda and Kenya (CHAI-III).

[12] Ampadu, B. (2021). Overview of hydrological and climatic studies in Africa: The case of Ghana. Cogent Engineering, 8(1), 1914288.

[13] Nicholson, S. E. (2017). Climate and climatic variability of rainfall over eastern Africa. Reviews of Geophysics, 55(3), 590-635.